Placement Control of Nanomaterial Arrays on the Surface-Reconstructed Block Copolymer Thin Films

Jeong Gon Son,[†] Wan Ki Bae,[†,⊥] Huiman Kang,[‡] Paul F. Nealey,[‡] and Kookheon Char[†,*]

[†]School of Chemical and Biological Engineering, Center for Functional Polymer Thin Films, and [⊥]School of Electrical Engineering and Computer Science, Seoul National University, Seoul, 151-744, Korea, and [‡]Department of Chemical and Biological Engineering, University of Wisconsin-Madison, Madison, Wisconsin 53706

ABSTRACT We present a control strategy for the facile placement of densely packed nanomaterial arrays (*i.e.*, nanoparticles and nanorods) on surface reconstructed polystyrene-*block*-poly(methyl methacrylate) thin film patterns. The surface reconstruction of perpendicularly oriented block copolymer thin films, which were produced by a treatment with selective solvent vapors for both blocks, created the topographical nanopatterns with enough height contrast for nanoparticle deposition without the need for additional selective etching of a single block domain. The deposition method of nanomaterials was also optimized, and densely packed one- and two-dimensional nanomaterials arrays in the grooves of the block copolymer film patterns were fabricated efficiently. Then, we demonstrated that height contrast of the surface reconstructed block copolymer films could be reversed by electron beam irradiation resulting in nanomaterial arrays placed at the mesa phase of the nanopatterns. On the basis of this nanomaterial placement control strategy, dual nanomaterial arrays on a single block copolymer pattern were also realized.

KEYWORDS: block copolymer · thin films · self-assembly · nanomaterial arrays · dual nanomaterials patterning

Nanomaterials such as metal and magnetic nanoparticles, semiconductor quantum dots, nanorods/wires, and carbon nanotubes have attracted considerable attention not only because of their unique electronic, optical, and magnetic properties originated from their size but also due to their extensive applications to optoelectronic devices, next-generation memory devices, and biological sensors.[1−5] To take full advantage of these unique properties for highly integrated fabrication, precise control of nanomaterial placement and its integration is essential. Although several methods for the controlled deposition of nanomaterials in nonconventional lithographic nanoscale patterns have been reported such as directed evaporation,[6−11] the use of an electrostatic interaction,[12] or applying magnetic-fields,[13] these approaches typically require additional elaborate and complicated procedures, deteriorating the merits (*i.e.*, cost effectiveness and ability to scale-up) of nanomaterials prepared by wet chemistry. Polymeric nanotemplates prepared from the microphase separation of block copolymers[14−18] can be a suitable alternative platform because the block copolymers form self-assembled nanostructures easily and cost-effectively over a large area with high fidelity, and their typical feature size is comparable to the characteristic size of the nanomaterials. Furthermore, block copolymers have recently been highlighted for the production of extraordinarily well-aligned and defect-free nanopatterns for real applications based on graphoepitaxy, directed assembly, and other methods.[15,19−21] Consequently, many studies have examined nanomaterial patterns based on block copolymer templates including the selective incorporation of nanoparticles into a single domain of a block copolymer matrix[16,22−24] and nanoparticles containing block copolymer micelle arrays.[25−27] Among them, nanomaterial partitioning on block copolymer thin film patterns has been studied extensively using a variety of methods including *in situ* synthesis of nanoparticle arrays[28−31] and the nanomaterial partitioning based on either the chemical difference in the patterns[32−34] or the topographical patterns in which one domain is selectively removed.[35,36] However, these deposition methods based on block copolymer templates have difficulty in controlling the placement of nanomaterials in the desired patterns and also have the drawback of possible nanomaterial aggregation due to various kinds of interactions among nanomaterials.

In the present study, we demonstrate a straightforward and reproducible method for controlling the arrangement of nanomaterial arrays on the block copolymer thin film patterns. This concept is based on the properties of surface reconstructed block copolymer thin films, which can be

*Address correspondence to khchar@plaza.snu.ac.kr.

Received for review August 2, 2009 and accepted November 8, 2009.

Published online November 16, 2009. 10.1021/nn900914q

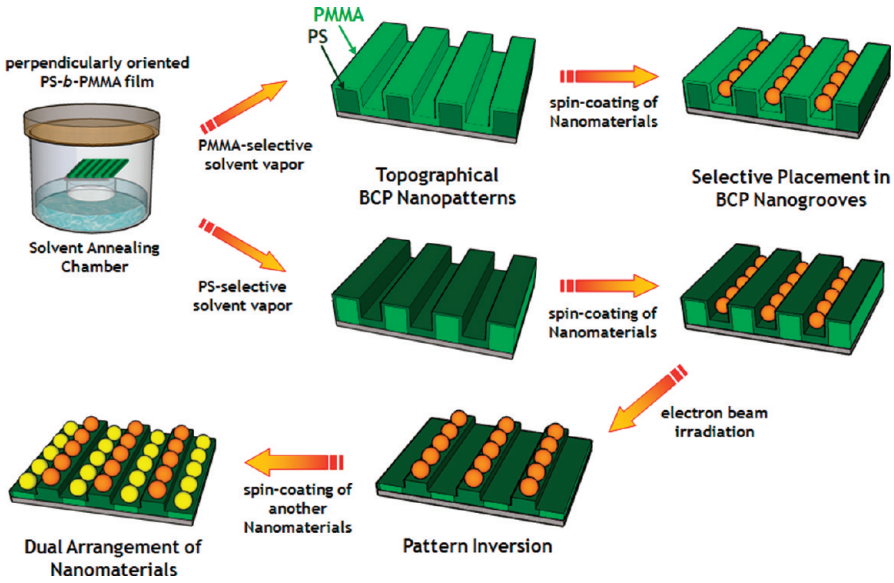

Figure 1. Schematic on the control of nanomaterial arrangements on patterned block copolymer thin films.

achieved by a treatment with solvent vapors that selectively swell the different blocks to create topographical nanopatterns coupled with electron beam irradiation to remove the blocks located in the mesa phase of these patterns. On these topographical patterns, densely packed nanomaterial patterns in the block grooves were achieved without massive aggregation of nanomaterials. In addition, inversion of the topographical BCP pattern heights was possible by electron beam irradiation, which was employed in this study to realize the nanomaterial arrays selectively located at the mesa phase of the patterns. We also demonstrate dual nanomaterial arrays in which two different nanomaterials are located in two different regions of the block patterns, as schematically shown in Figure 1.

RESULTS AND DISCUSSION

For the surface reconstructed block copolymer (BCP) film patterns, polystyrene-*block*-poly(methyl methacrylate) (PS-*b*-PMMA) with lamellar (52k−52k) and cylindrical (46k−21k) microphase-separated domains were used. Approximately 50 nm thick PS-*b*-PMMA films were first prepared by spin-coating onto PS-*random*-PMMA copolymer brushes grafted to Si wafers to achieve the perpendicular orientation of the block copolymer microdomains. For the nanoscale block copolymer line−space patterns, we employed the directed assembly of BCP films on chemically prepatterned Si wafers prepared by extreme-UV lithography.[19] These BCP films were then annealed at 190 °C in a vacuum oven for 72 h. Figure 2 panels a and b show atomic force microscopy (AFM) height images of perpendicularly ordered lamellar (Figure 2a) and cylindrical (Figure 2b) PS-*b*-PMMA block copolymer thin films. We note that these films are relatively flat with a height difference between the two different domains within 2 nm. These perpendicularly oriented films were then placed in a chamber saturated with a selective solvent vapor for a specific block of the BCP to induce the selective swelling of a single block domain. Since the swollen block was tethered to the other block in a block copolymer, lateral expansion of the nanopatterns was suppressed, and swollen block chains extended in the longitudinal direction and covered the surface of the films. When the treated film was removed from the solvent chamber, the solvent molecules evaporated quickly from the film, fixing the surface reconstructed morphology without any appreciable deswelling of the chains.

Several studies have examined the selective swelling of block copolymer thin films simply by dipping in a selective solvent.[37,38] However, the dipping method causes unnecessary roughening of the film surface and induces delamination of the BCP film from the substrate. In this study, the BCP film was exposed to a selective solvent vapor to achieve a surface reconstruction without causing significant random surface roughness, which is unsuitable for the nanomaterial patterning. In the case of a BCP film treated with a PMMA-selective solvent vapor such as acetic acid, the lamellar-forming block copolymer films formed topographical patterns with a height difference of 15 nm without altering the pattern pitch (Figure 2c). In the case of the cylinder-forming BCP films (*i.e.*, PS matrix with PMMA cylinders), vertically oriented PMMA cylinders were lowered forming a hole structure (Figure 2d). This result was explained by the acetic acid vapor selectively swelling the PMMA cylindrical domains and PMMA chains migrating from their phase to the surface. On the other hand, when the films were exposed to a PS-selective solvent vapor, such as cyclohexane, the lamellar BCP film yielded topographical patterns with 9 nm of height contrast (Figure 2e) and the BCP film with vertically oriented PMMA cylinders showed protruded island PMMA patterns with respect to the swollen PS matrix (Figure 2f) due to selective swelling of the PS domains. Based on the AFM results shown in Figure 2, the swollen block domains occupied the lower region in the topographical patterns.

To analyze the surface composition of the surface reconstructed BCP films, X-ray photoelectron spectroscopy (XPS) was employed. The XPS measurements were taken at a 15° takeoff angle to collect the information from the surface (*i.e.* the penetration depth is approximately 1.5 nm from the surface). Table S1 in the Supporting Information shows the XPS results on the

atomic composition of the BCP surface as well as the estimated block ratio exposed to the surface. The surface composition of the perpendicularly oriented pristine lamellar BCP film was approximately half of PS and the other half of PMMA. In contrast, the surface composition of the BCP film treated with acetic acid was dominant with the PMMA chains. This result confirms that the surface of the BCP film was almost entirely covered with swollen PMMA. In the case of the BCP film treated with cyclohexane, the surface composition of the PS block was over 90 mol % and the film was completely covered by swollen PS domains. Based on the AFM topography as well as the XPS analysis, the surface reconstruction of perpendicularly oriented BCP films treated by selective solvent vapors creates the topological patterns, covering the film surface entirely with swollen domains, as schematically shown in Figure 1.

The nanomaterial deposition process is also an important step toward realizing the selective nanomaterial array patterns. For typical nanomaterial arrays, several parameters for the nanomaterial deposition process should be considered. The first is the nanomaterial size, shape, and surface properties. Thus, several kinds of nanomaterials were prepared, such as CdSe@ZnS quantum dots (QDs), γ-Fe_2O_3 nanoparticles (NPs), and 1-D ZnO nanorods. CdSe@ZnS QDs with a diameter of 6 nm were mainly employed for patterning on perpendicularly oriented BCP substrates. Monodisperse 6 nm CdSe@ZnS QDs were synthesized based on our previously reported method[39,40] and monodisperse 9 nm γ-Fe_2O_3 NPs were prepared according to the procedure reported by Hyun *et al.*[41] The ZnO nanorods, with an average width and length of 10 and 80 nm, respectively, were also synthesized on the basis of the procedure reported by Sun *et al.*[42] The surfaces of CdSe@ZnS QDs and γ-Fe_2O_3 NPs were passivated with oleic acids while the surface of the ZnO nanorods was encapsulated with oleylamines to disperse the nanomaterials in organic solvents such as hexane, chloroform, and toluene. A linear hydrocarbon solvent, such as hexane, was chosen to disperse the nanomaterials because it is a nonsolvent (or poor solvent) for both PS and PMMA blocks while, at the same time, it is a good solvent for the nanomaterials tested in this study. Consequently, the block copolymer film structure is not seriously affected during spin-coating with hexane.

Second, selection of the nanomaterial deposition method is another important factor for obtaining well-defined nanomaterial arrays. While dip-coating is relatively slow and requires a large amount of nanomaterial solution, spin-coating is fairly simple and fast, requiring only a small amount of nanomaterial solution to cover a large area with good reproducibility. Accordingly, the spin-coating method has been used to deposit nanomaterials on the block copolymer patterns in many cases.[10,36,43,44] Therefore, the spin-casting method was employed in the present study. During

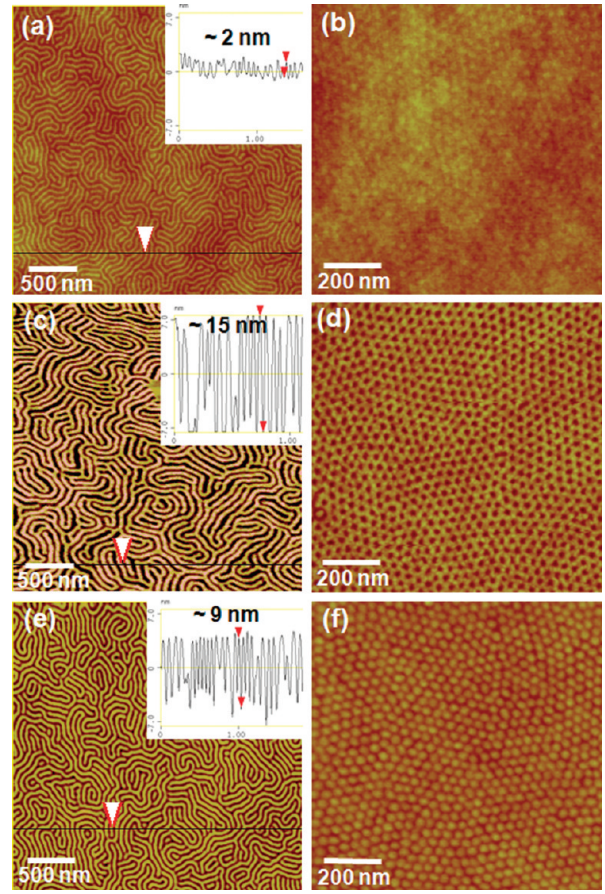

Figure 2. AFM topographic images of PS-*b*-PMMA thin films with perpendicularly oriented lamellar (a, c, and e) and cylindrical (b, d, and f) microdomains before (a and b) and after treatments with selective solvent vapors, (c and d) with PMMA-selective acetic acid vapor, and (e and f) with PS-selective cyclohexane vapor).

the spin-coating of a nanomaterial solution, various external interactions including the evaporation-induced capillary force, lateral centrifugal force, van der Waals force, thermal fluctuation, and physical confinement of the patterns can affect the deposition of nanomaterials in the patterned grooves.[7] In the case of colloidal suspensions as small as quantum dots, the evaporation-induced capillary force is the dominant force driving the nanomaterials to locate in the grooves of the topographical patterns.[7,10,44] The spin-coating process generally involves the two stages: solvent dispersion and evaporation.[44,45] At the initial stage of spin-coating, strong lateral centrifugal force quickly sweeps away the nanomaterials from the patterns. At the later stage of spin-casting when a significant amount of solvent evaporates, the remaining nanomaterials form contact lines with thin layers of solvent and, thus, the capillary force originating from the distorted contact angles drags the nanomaterials into groove patterns since the capillary force is particularly effective in the topographical BCP patterns. Consequently, nanomaterial arrays selectively located in the grooves of the pattern can be achieved. From experimental perspectives, factors such

as the nanomaterial concentration, solvent volatility, spin speed, and the relative size of topographical patterns compared with the nanomaterial size are also important for yielding well-defined nanomaterial arrays. In this study, 0.05−0.1 wt % of nanomaterial solutions in hexane was typically used for spin-coating at 1500 rpm on various types of BCP films.

The QDs prepared in present study were deposited on the BCP patterns in several different ways: (1) direct deposition on a perpendicularly oriented pristine BCP film without prior solvent annealing; (2) deposition on vertically oriented BCP thin films after UV irradiation to selectively remove the PMMA domains followed by rinsing with acetic acid; and (3) deposition on vertically oriented BCP films pretreated with either acetic acid or cyclohexane vapor. The direct deposition of QDs on a perpendicularly oriented pristine BCP film (see Figure S1a in Supporting Information) showed that a majority of QDs were located in the lower region of the BCP patterns but a significant degree of QD aggregation was observed because we believe that the capillary force among QDs is dominant over the capillary action between the QDs and shallow nanogrooves (with ~2 nm depth). The QDs were also deposited on a patterned BCP film treated with UV-irradiation followed by rinsing with acetic acid (see also Figure S1b in Supporting Information). After selective removal of the PMMA domains following this treatment procedure, the film contained 1:1 line and space patterns with 24 nm in width and 50 nm in depth, which is equivalent to the film thickness. In this case, the QDs were mainly located in the grooves but not densely packed to yield well-defined QD arrays along the BCP patterns, presumably because the size (width) of the grooves was fairly larger than the QD size and the sidewalls of the groove patterns were quite steep.

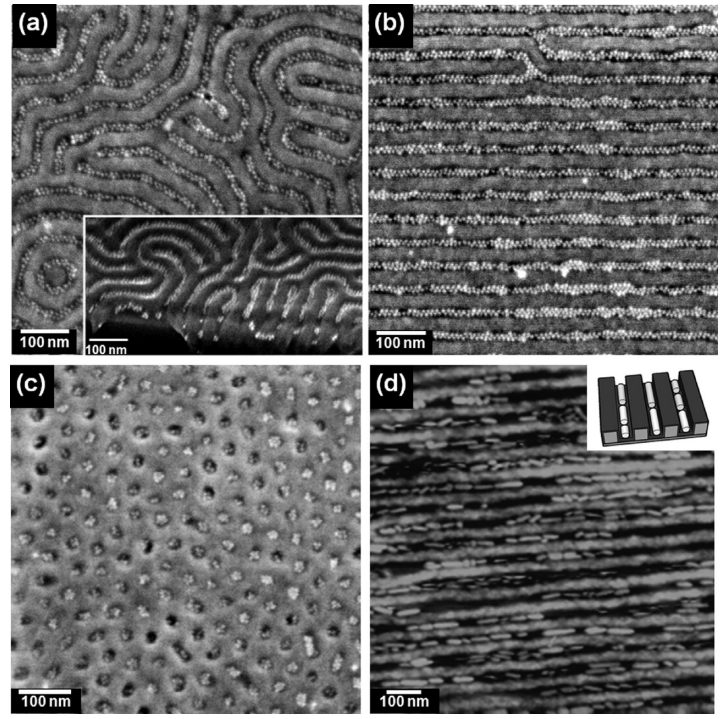

Figure 3. Microscopic images of nanomaterials deposited on the surface reconstructed PS-*b*-PMMA block copolymer thin films with perpendicular orientation after the solvent treatment with PMMA-selective acetic acid. FE-SEM images of CdSe@ZnS QDs located in the nanoscale-grooves in (a) randomly oriented lamellar, (b) one-dimensional (1D) directed-assembled lamellar, and (c) cylindrical morphology, and (d) the AFM image of well aligned 1-D ZnO nanorods arrays placed in the nanoscale-grooves in 1D directed-assembled lamellar morphology BCP pattern.

In contrast, CdSe@ZnS QDs were densely packed into the grooves on the BCP film patterns treated with acetic acid vapor (Figure 3a) and we note that the selectivity of the QDs located in the grooves was almost 99.9%. Ultimately, the QD line arrays could be realized on a one-dimensional (1D) directed self-assembled lamellar BCP film, as shown in Figure 3b. In these QD arrays, the QD density is estimated to be approximately 3600 clusters/μm^2, which is comparable to the value for a closely packed QD monolayer on a substrate. The reason of these highly selective and dense nanomaterials patterns is that one of the domain in the surface reconstructed BCP film was not removed but selectively swollen and the film formed a topographical pattern with the depth and width of the grooves comparable to the QD size. Two-dimensional (2D) QD dot patterns were also demonstrated with cylinder-forming BCP films treated with acetic acid vapor, as can be seen in Figure 3c. To apply this deposition method to 1D nanomaterials, ZnO nanorods, 10 nm in diameter and 80 nm in length, were deposited using the same procedure. The ZnO nanorods were well sequestered into the nanogrooves formed on a 1D directed self-assembled lamellar block copolymer thin film treated with acetic acid vapor, as shown in Figure 3d. It is found that the selectivity of nanorods located in the grooves was over 99% and the nanorod density was approximately 500 nanorods/μm^2. In addition, we discovered that the high aspect ratio nanorods were much better aligned with the pattern direction while the low aspect ratio nanorods residing in the grooves were somewhat tilted. The regions where the nanorods are doubly aligned in a single groove also were observed since the diameter was approximately 10 nm while the width of the grooves was around 24 nm.

In the case of a BCP film annealed with cyclohexane vapor, we observed with AFM that the CdSe@ZnS QDs were selectively located in the PS-covered grooves of BCP topographical patterns (Figure 4a). What is strik-

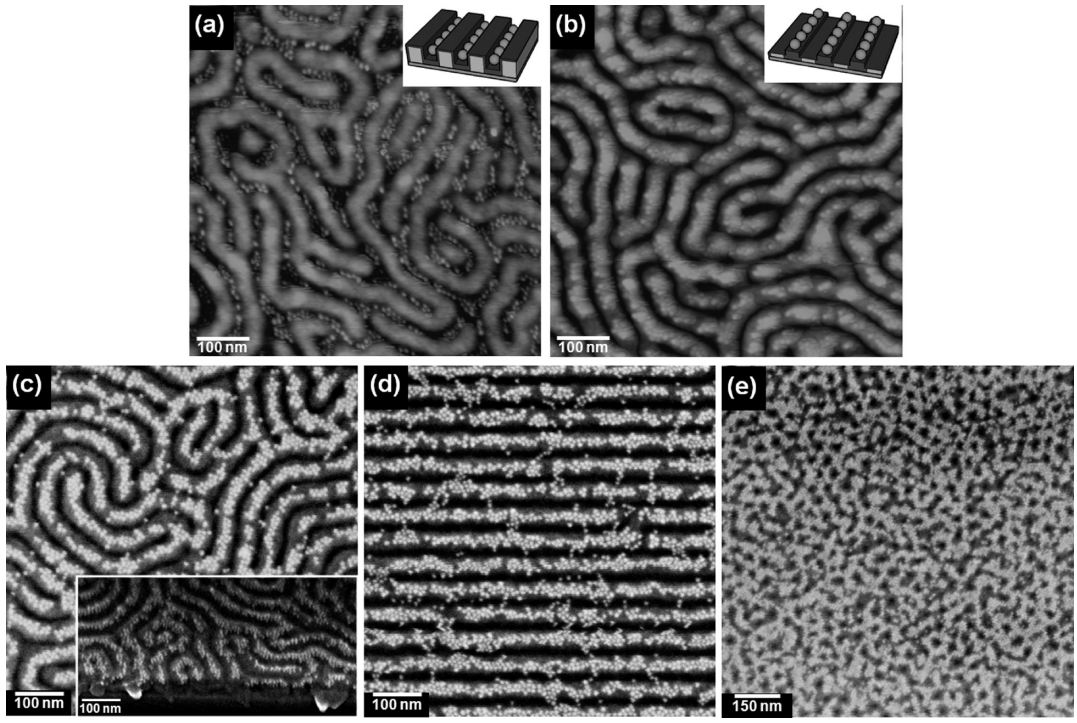

Figure 4. CdSe@ZnS QDs deposited on perpendicularly oriented lamellar PS-*b*-PMMA thin films treated with PS-selective cyclohexane vapor. (a) The AFM image of CdSe@ZnS QD arrays on cyclohexane vapor treated films. The image shows that QDs selectively located in the nanogrooves of the pattern. (b) The AFM image of CdSe@ZnS QDs deposited on the patterns after exposed to the electron beam irradiation. Note that the QDs reside at the mesa of the topographical patterns. (c−e) The FE-SEM images of CdSe@ZnS QD arrays placed in cyclohexane vapor treated (c) randomly oriented lamellar, (d) 1D directed-assembled lamellar, and (e) cylindrical morphology of perpendicularly oriented block copolymer thin films after exposure to electron beam irradiation.

ingly interesting, however, is the observation that the cyclohexane vapor-treated BCP film with irradiation-labile PMMA domains (with a thin layer of PS blocks) on top of the patterns caused an inversion in domain height when the BCP sample was irradiated with an electron beam. It is well-known that when an electron beam impinges on polymer surfaces, it causes chemical changes in the polymeric samples (e.g., the degradation for the PMMA block and cross-linking for the PS block of PS-*b*-PMMA block copolymer upon electron beam irradiation).[46,47] Consequently, the flat film orientation of PS-*b*-PMMA can be easily examined by FE-SEM, of which the electron beam selectively degrades the PMMA domain, enabling the topographical change in the patterns.[18,19] To verify the effect of electron beam irradiation on a QD-aligned BCP thin film, the film was first subject to the electron beam irradiation with FE-SEM (5 kV and 20 μA for 10 min; 7×10^{20} e/cm^2), and the topography of the BCP film in the irradiated region was then examined by AFM, as shown in Figure 4b. It is interesting to note that the QDs were now exclusively located at the mesa phase of the patterns. This observation suggests that when cyclohexane vapor-treated topographical BCP patterns with PMMA domains located higher than PS domains is exposed to an electron beam, the height of the PMMA domains selectively decreases compared with the PS domains, resulting in an inversion of the domain height in topographical patterns. As a consequence, FE-SEM showed that the QD arrays were selectively located at the mesa phase of topographical patterns of lamellae-forming BCP films (Figure 4c), direct self-assembled 1-D lamellar BCP films (Figure 4d) and the 2D QD cross network structure obtained on cylinder-forming BCP patterns, as shown in Figure 4e. These experimental results clearly demonstrate that the placement of nanomaterials on topographical BCP patterns can

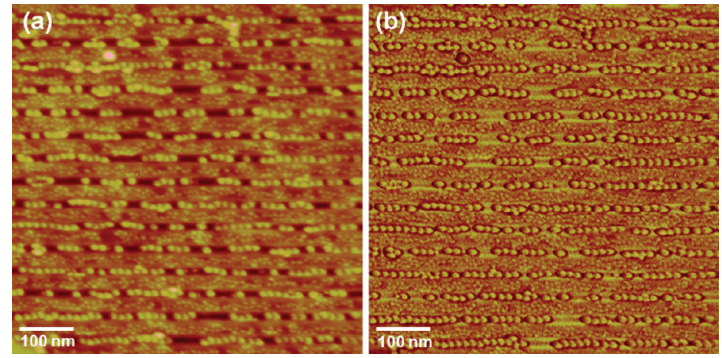

Figure 5. The AFM images of dual patterned nanomaterials on PS-*b*-PMMA thin films with 1D directed-assembled lamellar morphology. CdSe@ZnS QDs (with a diameter of 6 nm) resides at the mesa of patterns while γ-Fe_2O_3 NPs (with a diameter of 9 nm) are located in the nanogrooves: (a) height image and (b) phase image.

be easily controlled using a vapor treatment with a selective solvent(s) coupled with electron beam irradiation.

The nanomaterial placement control, introduced in the present study, can be extended to the fabrication of dual nanomaterial arrays. Nanoparticles with two different sizes (*i.e.*, CdSe@ZnS QDs with 6 nm in diameter and γ-Fe_2O_3 NPs with 9 nm in diameter) were employed to realize dual array patterning on a perpendicularly oriented BCP substrate. The vertically oriented block copolymer film was first treated with cyclohexane vapor to amplify the topographical patterns. The substrate was then spin-coated with QDs followed by electron beam irradiation (at 5 kV and 20 μA for 10 min: 7×10^{20} e/cm^2) to form QD arrays at the PS mesa phase of the patterns. γ-Fe_2O_3 NPs dissolved in hexane were then spin-coated onto the BCP patterns containing the QD arrays. After the second spin-coating, the γ-Fe_2O_3 NPs were selectively located in the PMMA grooves without perturbing the QD arrays situated in the PS mesa phase, as shown in Figure 5 for the directed self-assembled 1D lamellar structure. We believe that the QDs were attached to the PS domains during electron beam irradiation, keeping the QD arrays from being removed during the second spinning. In addition, we note that each nanoparticle (6 nm QDs and 9 nm NPs) was well sequestered onto each block domain without interference between the two domains. Overall, the ability to control the placement of two different nanomaterials in specific positions of the BCP nanodomains, as demonstrated in this study, will open up a new avenue for high density devices with multiple functions.

CONCLUSION

The selective partitioning and placement control of nanomaterials on nanosized surface patterns of topographically reconstructed PS-*b*-PMMA thin films were achieved. The topographical reconstruction of a BCP film without an etching process was realized by vapor treatment with a selective solvent for each block. Based on these surface-reconstructed BCP films, well-ordered and densely packed 1D nanomaterial arrays were obtained by simply spin-coating a variety of nanomaterials. Another particularly important and useful aspect was that the reconstructed BCP films with PMMA blocks located at the mesa phase of the patterns led to an inversion of the pattern height upon electron beam treatment, such that QDs, initially placed in the nanogrooves of the BCP domains, were selectively located in the PS mesa phase of the BCP patterns upon treatment. Moreover, versatile control of the placement of nanomaterials on BCP topographical patterns, combining the vapor treatment with a selective solvent, spin-coating, and electron beam irradiation, was even extended to producing dual nanomaterial arrays on highly aligned one-dimensional BCP topographical patterns. Since perfectly aligned and defect-free nanopatterns for real device applications have recently been developed using BCP film technology, the simplicity for placement control and dual nanomaterial arrays based on the BCP films introduced in the present study highlight a wide range of new applications such as high density devices with multiple (*i.e.*, coupled electronic, photonic, plasmonic, and so forth) functions.

EXPERIMENTAL METHODS

Materials. Polystyrene-*block*-poly(methyl methacrylate) (PS-*b*-PMMA) diblock copolymers were purchased from Polymer Source. The molecular weight of the symmetric diblock copolymer was 104 kg/mol (52k−52k) with a polydispersity index of 1.09 and that of the asymmetric diblock copolymer was 67 kg/mol(46k−21k) with a polydispersity index of 1.09. The average domain spacings (L_0) measured by small-angle X-ray scattering (SAXS) experiments were 47 and 24 nm, respectively. PS brushes (5k) and PS-*random*-PMMA brushes (5k, 58:42 fractions) were synthesized by atomic transfer radical polymerization (ATRP). CdSe@ZnS quantum dots (QDs) were prepared by the previous method.[39,40] The diameter of QDs was approximately 6 nm, all of which were capped with organic surfactant, oleic acid. For dual nanomaterial arrays, other nanomaterials used in the study, γ-Fe_2O_3 NPs, were synthesized using the procedure reported by Hyun and co-workers.[41] The size of the γ-Fe_2O_3 NPs was around 9 nm, and they were also capped with oleic acids. We also prepared one-dimensional nanomaterial, ZnO nanorods, which were produced using the procedure reported by Sun *et al.*[42] and were approximately 80 nm long and 10 nm wide.

Topographical Patterns of Block Copolymer Thin Film. SiO_x/Si substrates were spin-coated by 1 wt % PS-*random*-PMMA copolymer brush solution in toluene and annealed at 190 °C for 2 days in vacuum. The substrates were then rinsed using toluene to remove weakly physisorbed copolymer chains. For 1-D patterns, extreme-UV patterned on PS brushes grafted to the SiO_x/Si substrates were performed as previously described methods.[19] The 1 wt % PS-*b*-PMMA in toluene was deposited by spin-coating on brush attached substrates and the film was annealed at 190 °C for 2 days to form perpendicular orientation of microdomains. Perpendicularly ordered block copolymer films were then exposed to the saturated solvent vapor (acetic acid or cyclohexane) during 1 h to induce the selective swelling of one domain of the block copolymer. Topographical morphology of the selective swelled films were investigated by atomic force microscopy (AFM, Digital Instrument, Nanoscope IIIA) in tapping mode and surface composition of the film analyzed by X-ray photoelectron spectroscopy (XPS, KRATOS, AXIS). Spectra were obtained at a 15° takeoff angle, corresponding to ~1.5 nm sampling depth.

Nanomaterials Patterns on Block Copolymer Thin Film. Oleic acid or oleylamine-stabilized nanomaterials were dispersed in hexane with 0.05−0.1 wt % concentration. The nanomaterials solution was then spin-coated on topographically patterned block copolymer thin films at 1500 rpm. The morphology of nanomaterials patterns was observed by field emission-scanning electron microscope (FE-SEM, LEO 1550-VP) operated at 1 kV and AFM. During the use of FE-SEM, electron beam irradiated the film and induced an electro-thinning effect on PMMA segments. Particularly, the electron beam caused the reversing of the pattern location of the cyclohexane-treated topographical patterns. For dual nanomaterials patterns, we spin-coated another nanomaterials solution on electron beam irradiated nanomaterials patterns.

Acknowledgment. This work was financially supported by the Korea Science and Engineering Foundation (KOSEF) grant through the Acceleration Research (R17-2007-059-01000-0) and the NANO Systems Institute-National Core Research Center (R15-2003-032-02002-0) funded by the Ministry of Education, Science and Technology (MEST) of Korea. We also acknowledge the financial support from the MEST on graduate programs at Seoul National University through the Brain Korea 21 Program and the World Class University (WCU) Program of Chemical Convergence for Energy and Environment (C2E2; 400-2008-0230). Additional financial support by the Korean Ministry of Knowledge and Economy (MKE) through the System IC 2010 Project is greatly acknowledged. P. F. Nealey and H. Kang are grateful for the financial support from the Semiconductor Research Corporation and the National Science Foundation through the Nanoscale Science and Engineering Center (NSEC) at the University of Wisconsin (DMR-0425880).

Supporting Information Available: XPS analysis of the vapor-treated BCP films and FE-SEM images of nanomaterials deposited on conventionally treated BCP films. This material is available free of charge *via* the Internet at http://pubs.acs.org.

REFERENCES AND NOTES

1. Bronstein, L.; Antonietti, M.; Valetsky P. Metal Colloids in Block Copolymer Micelles: Formation and Material Properties. In *Nanoparticles and Nanostructured Films*; Fendler, J. H., Eds.; Wiley-VCH: Weinheim, Germany, 1998; pp 145−172.
2. Alivisatos, A. P. Semiconductor Clusters, Nanocrystals, and Quantum Dots. *Science* **1996**, *271*, 933–937.
3. Murray, C. B.; Kagan, C. R.; Bawendi, M. G. Synthesis and Characterization of Monodisperse Nanocrystals and Close-Packed Nanocrystal Assemblies. *Annu. Rev. Mater. Sci.* **2000**, *30*, 545–610.
4. Sun, S. H.; Murray, C. B.; Weller, D.; Folks, L.; Moser, A. Monodisperse FePt Nanoparticles and Ferromagnetic FePt Nanocrystal Superlattices. *Science* **2000**, *287*, 1989–1992.
5. Geissler, M.; Xia, Y. N. Patterning: Principles and Some New Developments. *Adv. Mater.* **2004**, *16*, 1249–1269.
6. Cui, Y.; Bjork, M. J.; Liddle, J. A.; Sonnichsen, C.; Boussert, B.; Alivisatos, A. P. Integration of Colloidal Nanocrystals into Lithographically Patterned Devices. *Nano Lett.* **2004**, *4*, 1093–1098.
7. Liddle, J. A.; Cui, Y.; Alivisatos, A. P. Lithographically Directed Self-Assembly of Nanostructures. *J. Vac. Sci. Technol., B* **2004**, *22*, 3409–3414.
8. Kraus, T.; Malaquin, L.; Schmid, H.; Riess, W.; Spencer, N. D.; Wolf, H. Nanoparticle Printing with Single-Particle Resolution. *Nat. Nanotechnol.* **2007**, *2*, 570–576.
9. Santhanam, V.; Andres, R. P. Microcontact Printing of Uniform Nanoparticle Arrays. *Nano Lett.* **2004**, *4*, 41–44.
10. Xia, D.; Biswas, A.; Li, D.; Brueck, S. R. J. Directed Self-Assembly of Silica Nanoparticles into Nanometer-Scale Patterned Surfaces Using Spin-Coating. *Adv. Mater.* **2004**, *16*, 1427–1432.
11. Spatz, J. P.; Chan, V. Z.; Mossmer, S.; Kamm, F.; Plttl, A.; Ziemann, P.; Moller, M. A Combined Top-Down/Bottom-Up Approach to the Microscopic Localization of Metallic Nanodots. *Adv. Mater.* **2002**, *14*, 1827–1832.
12. Bezryadin, A.; Dekker, C.; Schmid, G. Electrostatic Trapping of Single Conducting Nanoparticles between Nanoelectrodes. *Appl. Phys. Lett.* **1997**, *71*, 1273–1275.
13. Lee, C. S.; Lee, H.; Westervelt, R. M. Microelectromagnets for the Control of Magnetic Nanoparticles. *Appl. Phys. Lett.* **2001**, *79*, 3308–3310.
14. Lazzari, M.; Lopes-Quintela, M. A. Block Copolymer as a Tool for Nanomaterial Fabrication. *Adv. Mater.* **2003**, *15*, 1583–1594.
15. Cheng, J. Y.; Ross, C. A.; Smith, H. I.; Thomas, E. L. Templated Self-Assembly of Block Copolymers: Top-Down Helps Bottom-Up. *Adv. Mater.* **2006**, *18*, 2505–2521.
16. Bockstaller, M. R.; Mickiewicz, R. A.; Thomas, E. L. Block Copolymer Nanocomposite: Perspective for Tailored Functional Materials. *Adv. Mater.* **2005**, *17*, 1331–1349.
17. Darling, S. B. Directing the Self-Assembly of Block Copolymers. *Prog. Polym. Sci.* **2007**, *32*, 1152–1204.
18. Son, J. G.; Bulliard, X.; Kang, H.; Nealey, P. F.; Char, K. Surfactant-Assisted Orientation of Thin Diblock Copolymer Films. *Adv. Mater.* **2008**, *20*, 3643–3648.
19. Kim, S. O.; Solak, H. H.; Stoykovich, M.P.; Ferrier, N. J.; de Pablo, J. J.; Nealey, P. F. Epitaxial Self-Assembly of Block Copolymers on Lithographically Defined Nanopatterned Substrates. *Nature* **2003**, *424*, 411–414.
20. Ruiz, R.; Kang, H.; Detcheverry, F. A.; Dobisz, E.; Kercher, D. S.; Albrecht, T. R.; de Pablo, J. J.; Nealey, P. F. Density Multiplication and Improved Lithography by Directed Block Copolymer Assembly. *Science* **2008**, *321*, 936–939.
21. Bita, I.; Yang, J. K. W.; Jung, Y. S.; Ross, C. A.; Thomas, E. L.; Berggren, K. K. Graphoepitaxy of Self-Assembled Block Copolymers on Two-Dimensional Periodic Patterned Templates. *Science* **2008**, *321*, 939–943.
22. Bockstaller, M. R.; Lapetnikov, Y.; Margel, S.; Thomas, E. L. Size-Selective Organization of Enthalpic Compatibilized Nanocrystals in Ternary Block Copolymer/Particle Mixtures. *J. Am. Chem. Soc.* **2003**, *125*, 5276–5277.
23. Chiu, J. J.; Kim, B. J.; Kramer, E. J.; Pine, D. J. Control of Nanoparticle Location in Block Copolymers. *J. Am. Chem. Soc.* **2005**, *127*, 5036–5037.
24. Tsutusmi, K.; Funaki, Y.; Hirokawa, Y.; Hashimoto, T. Selective Incorporation of Palladium Nanoparticles into Microphase-Separated Domains of Poly(2-vinylpyridine) - *block*-polyisoprene. *Langmuir* **1999**, *15*, 5200–5203.
25. Spatz, J. P.; Mossmer, S.; Hartmann, C.; Moller, M.; Herzog, T.; Krieger, M.; Boyen, H.-G.; Ziemann, P.; Kabius, B. Ordered Deposition of Inorganic Clusters from Micellar Block Copolymer Films. *Langmuir* **2000**, *16*, 407–415.
26. Boontongkong, Y.; Cohen, R. E. Cavitated Block Copolymer Micellar Thin Films: Lateral Arrays of Open Nanoreactors. *Macromolecules* **2002**, *35*, 3647–3652.
27. Sohn, B.; Choi, J.; Yoo, S. I.; Yun, S.; Zin, W.; Jung, J. C.; Kanehara, M.; Hirata, T.; Teranishi, T. Directed Self-Assembly of Two Kinds of Nanoparticles Utilizing Monolayer Films of Diblock Copolymer Micelles. *J. Am. Chem. Soc.* **2003**, *125*, 6368–6369.
28. Lopes, W. A.; Jaeger, H. M. Hierarchical Self-Assembly of Metal Nanostructures on Diblock Copolymer Scaffolds. *Nature* **2001**, *414*, 735–738.
29. Horiuchi, S.; Sarwar, M. I.; Nakao, Y. Nanoscale Assembly of Metal Clusters in Block Copolymer Films with Vapor of a Metal−Acetylacetonato Complex Using a Dry Process. *Adv. Mater.* **2000**, *12*, 1507–1511.
30. Sohn, B. H.; Seo, B. H. Fabrication of the Multilayered Nanostructure of Alternating Polymers and Gold Nanoparticles with Thin Films of Self-Assembling Diblock Copolymers. *Chem. Mater.* **2001**, *13*, 1752–1757.
31. Li, J.; Kamata, K.; Watanabe, S.; Iyoda, T. Template- and Vacuum-Ultraviolet-Assisted Fabrication of a Ag−Nanoparticle Array on Flexible and Rigid Substrates. *Adv. Mater.* **2007**, *19*, 1267–1271.
32. Zehner, R. W.; Lopes, W. A.; Morkved, T. L.; Jaeger, H.; Sita, L. R. Selective Decoration of a Phase-Separated Diblock Copolymer with Thiol-Passivated Gold Nanocrystals. *Langmuir* **1998**, *14*, 241–244.
33. Shenhar, R.; Jeoung, E.; Srivastava, S.; Norsten, T. B.; Rotello, V. M. Crosslinked Nanoparticle Stripes and Hexagonal Networks Obtained *via* Selective Patterning of Block Copolymer Thin Films. *Adv. Mater.* **2005**, *17*, 2206–2210.
34. Watanabe, S.; Fujiwara, R.; Hada, M.; Okazaki, Y.; Iyoda, T. Site-Specific Recognition of Nanophase-Separated Surfaces of Amphiphilic Block Copolymers by Hydrophilic and Hydrophobic Gold Nanoparticles. *Angew. Chem., Int. Ed.* **2007**, *46*, 1120–1123.
35. Misner, M. J.; Skaff, H.; Emrick, T.; Russell, T. P. Directed Deposition of Nanoparticles Using Diblock Copolymer Templates. *Adv. Mater.* **2003**, *15*, 221–224.

36. Darling, S. B.; Yufa, N. A.; Cisse, A. L.; Bader, S. D.; Sibener, S. J. Self-Organization of FePt Nanoparticles on Photochemically Modified Diblock Copolymer Templates. *Adv. Mater.* **2005**, *17*, 2446–2450.
37. Xu, T.; Stevens, J.; Villa, J. A.; Goldbach, J. T.; Guarini, K. W.; Black, C.T.; Hawker, C. J.; Russell, T. P. Block Copolymer Surface Reconstuction: A Reversible Route to Nanoporous Films. *Adv. Funct. Mater.* **2003**, *13*, 698–702.
38. Xu, C.; Fu, X.; Fryd, M.; Xu, S.; Wayland, B. B.; Winey, K. I.; Composto, R. J. Reversible Stimuli-Responsive Nanostructures Assembled from Amphiphilic Block Copolymers. *Nano Lett.* **2006**, *6*, 282–287.
39. Bae, W. K.; Char, K.; Hur, H.; Lee, S. Single-Step Synthesis of Quantum Dots with Chemical Composition Gradients. *Chem. Mater.* **2008**, *20*, 531–539.
40. Bae, W. K.; Nam, M. K.; Char, K.; Lee, S. Gram-Scale One-Pot Synthesis of Highly Luminescent Blue Emitting $Cd_{1-x}Zn_xS$/ZnS Nanocrystals. *Chem. Mater.* **2008**, *20*, 5307–5313.
41. Park, J.; An, K.; Hwang, Y.; Park, J.; Noh, H.; Kim, J.; Park, J.; Hwang, N.; Hyeon, T. Ultra-Large-Scale Syntheses of Monodisperse Nanocrystals. *Nat. Mater.* **2004**, *3*, 891–895.
42. Sun, B.; Sirringhaus, H. Solution-Processed Zinc Oxide Field-Effect Transistors Based on Self-Assembly of Colloidal Nanorods. *Nano Lett.* **2005**, *5*, 2408–2413.
43. Darling, S. B. Mechanism for Hierarchical Self-Assembly of Nanoparticles on Scaffolds Derived from Block Copolymers. *Surf. Sci.* **2007**, *601*, 2555–2561.
44. Mertens, K.; Putkaradze, V.; Xia, D.; Brueck, S. R. J. Theory and Experiment for One-Dimensional Directed Self-Assembly of Nanoparticles. *J. Appl. Phys.* **2005**, *98*, 034309.
45. Zhao, Y.; Marshall, J. S. Spin Coating of a Colloidal Suspension. *Phys. Fluids* **2008**, *20*, 043302.
46. Lee, H. M.; Kim, Y. N.; Kim, B. H.; Kim, S. O.; Cho, S. O. Fabrication of Luminescent Nanoarchitectures by Electron Irradiation of Polystyrene. *Adv. Mater.* **2008**, *20*, 2094–2098.
47. Darling, S. B.; Hoffmann, A. Tuning Metal Surface Diffusion on Diblock Copolymer Films. *J. Vac. Sci. Technol., A* **2007**, *25*, 1048–1051.